Inactivation of the PD-1-dependent immunoregulation in mice exacerbates contact hypersensitivity resembling immune-related adverse events.

(PD-1 依存的な免疫制御機構の抑制は、免疫関連副作用に類似する接触性皮膚炎の悪化を引き起こす)

Matin Dokht Ashoori

Inactivation of the PD-1-dependent immunoregulation in mice exacerbates contact hypersensitivity resembling immune-related adverse events

Matin Dokht Ashoori[1,2], Kensuke Suzuki[1,3], Yosuke Tokumaru[1,3], Naoko Ikuta[1], Masaki Tajima[1], Tasuku Honjo[2], and Akio Ohta[1*]

[1] Department of Immunology, Foundation for Biomedical Research and Innovation at Kobe, Kobe, Japan
[2] Department of Immunology and Genomic Medicine, Graduate School of Medicine, Kyoto University, Kyoto, Japan
[3] Pharmaceutical Research Labs, Meiji Seika Pharma Co., Ltd., Yokohama, Japan

* Correspondence: Akio Ohta (ohta-a@fbri.org)

Keywords: PD-1, cancer immunotherapy, immune-related adverse events, contact hypersensitivity, skin, T cells, CXCR3

Running title: Exacerbated dermatitis in PD-L1 blockade

Abstract

Blockade of PD-1, an indispensable physiological immunoregulatory mechanism, enhances immune activities and is widely used in the immunotherapy of cancer. This treatment often accompanies inflammatory complication called immune-related adverse events (irAE), most frequently in the skin. To analyze how skin inflammation develops by the blockade of PD-1-dependent immunoregulation, we studied the exacerbation of oxazolone-induced contact hypersensitivity by PD-L1 blockade. The inactivation of PD-1 signaling enhanced swelling of the skin with massive $CD8^+$ T cell infiltration. Among PD-1-expressing cells, T cells were the predominant targets of anti-PD-L1 mAb treatment since PD-L1 blockade did not affect skin inflammation in $RAG2^{-/-}$ mice. PD-L1 blockade during immunization with oxazolone significantly promoted the development of hapten-reactive T cells in the draining lymph nodes. The enhancement of local $CD8^+$ T cell-dominant immune responses by PD-L1 blockade was correlated with the upregulation of CXCL9 and CXCL10. Challenges with a low dose of oxazolone did not demonstrate any significant dermatitis; however, the influence of PD-L1 blockade on T cell immunity was strong enough to cause the emergence of notable dermatitis in this suboptimal dosing, suggesting its relevance to dermal irAE development. In the low-dose setting, the blockade of CXCR3, receptor of CXCL9/10, prevented the induction of T cell-dominant inflammation by anti-PD-L1 mAb. This experimental approach reproduced $CD8^+$ T cell-dominant form of cutaneous inflammation by the blockade of PD-L1 that has been observed in dermal irAE in human patients.

Introduction

The immune system has its own regulatory mechanisms with which the intensity of immune responses is modulated at proper levels. Since some of these mechanisms are exceptionally important, the deficiency of one of such immunoregulatory mechanisms may not be compensated by all of the rest. PD-1 represents the indispensable immunoregulatory mechanisms that spontaneously downregulate immune responses. When PD-1-expressing T cells recognize antigen presented on MHC, PD-1 interacts with PD-L1 or PD-L2 on their counterpart and triggers an inhibitory signal that interrupts T cell receptor signaling (Okazaki et al., 2013). PD-1 expression is not detectable in most resting T cells, but it is notably induced upon activation. This expression pattern indicates PD-1's function as a negative feedback mechanism in activated immune cells. The pathophysiological importance of PD-1 has been demonstrated in spontaneous pathogenesis of inflammatory diseases in PD-$1^{-/-}$ mice. Interestingly, PD-1-deficiency causes various autoimmune disease-like symptoms in different organs depending on the genetic strain of mice (Nishimura et al., 1999; Nishimura et al., 2001; Wang et al., 2005; Wang et al., 2010).

The major role of the PD-1-mediated regulation in the immune system led to the successful development of cancer immunotherapy. Blockade of the immunosuppressive signaling using anti-PD-1 mAb promoted anti-tumor immune responses and dramatically improved treatment of cancer patients including those who are not responding well to conventional treatments (Iwai et al., 2002; Topalian et al., 2012; Sanmamed and Chen, 2018; Chamoto et al., 2020). Although it is not very frequent, PD-1 blockade can cause inflammatory complications outside tumors. Such immune-related adverse events (irAE) in cancer patients can happen in various organs and in different forms of inflammation, e.g. self-reactive T cells and autoantibodies.

Cutaneous inflammation is the most common form of irAE (Michot et al., 2016; Young et al., 2018). Most cases of this form are not life-threatening, e.g. rash, alopecia and vitiligo. However, severe forms of cutaneous irAE are also reported in Stevens-Johnson syndrome and toxic epidermal necrolysis after the treatment with anti-PD-1 or anti-PD-L1 antibodies (Saw et al., 2017; Haratake et al., 2018; Salati et al., 2018; Coleman et al., 2020; Robinson et al., 2020). Histochemical examination of affected skins from cutaneous irAE patients demonstrated $CD8^+$ T cells accumulation and apoptotic keratinocytes, suggesting T cell-mediated pathophysiology (Goldinger et al., 2016). Levels of perforin and granzyme B were also found to increase in cutaneous irAE. Consistent with this observation, PD-$1^{-/-}$ T cells intensified allogenic reaction in mice and developed severe dermatitis accompanying extensive lymphocytes infiltration in the dermis (Nishimura et al., 1999). PD-L1 expression in keratinocytes can prevent T cell-dependent pathogenesis of dermatitis (Ritprajak et al., 2010; Okiyama and Katz, 2014).

To study the exaggeration of cutaneous inflammation by the blockade of PD-1 pathway, we used a contact hypersensitivity (CHS) model in mice. CHS is inducible by repeated exposure to a hapten, which induces proinflammatory activities of antigen-specific T cells (Honda et al., 2013). Depletion of $CD4^+$ and $CD8^+$ T cells is known to strongly impair CHS response. Prior to massive T cell accumulation, capillary vasodilation and neutrophils infiltration take place in the early phase of CHS. Keratinocytes recruit dendritic cells and neutrophils through the action of cytokines, chemokines and chemical mediators. These inflammatory responses by non-T cells cooperate with subsequent antigen-specific T cell responses in optimal CHS induction.

In this study, blockade of the PD-1 pathway using anti-PD-L1 mAb exaggerated CHS along with local $CD8^+$ T cell accumulation. The current study shows that T cells are the primary target of PD-1 blockade treatment in the enhancement of cutaneous inflammation. Upregulation of chemokines such as CXCL9 and CXCL10 was involved in the exacerbation of inflammation. The effect of PD-L1 blockade on T cell immunity was strong enough to cause the emergence of T cell-dominant dermatitis in the skin exposed to a suboptimal dose of hapten.

Materials and methods

Mice

Female C57BL/6 mice were purchased from Japan SLC Co. (Shizuoka, Japan). PD-$1^{-/-}$ mice and $RAG2^{-/-}$ mice with C57BL/6-background were bred in our animal facility. The animals were housed under specific pathogen-free conditions and used between 8 and 12 weeks of age. All experiments were conducted in accordance with the institutional animal care guidelines.

Induction of CHS

Female C57BL/6 mice were sensitized by topical application of 1 mg oxazolone (4-ethoxymethylene-2-phenyl-2-oxazolin-5-one; Sigma, St. Louis, MO) in 20 μl acetone/olive oil (4:1 vol/vol) on the shaved abdominal skin. Seven days later, mice were anesthetized with isoflurane to allow topical application of 20-200 μg oxazolone (10 μl) on the back side of the ear. Challenges were repeated every other day on day 9 and 11. The ear thickness was evaluated 48 h after each challenge using a digital thickness gauge (#547-301; Mitutoyo Corp., Kawasaki, Japan). On day 13, the ears were harvested from euthanized mice for further analysis.

Treatment with antibodies

To block PD-L1, mice received i.p. injections of anti-mouse PD-L1 mAb (1-111A; 0.3mg/mouse) immediately after the sensitization and on days 3, 7, 9 and 11. $CD8^+$ and $CD4^+$ T cells was depleted by injecting mice intraperitoneally with 0.2 mg of anti-CD8b (clone: 2.43; BioXCell, Lebanon, NH) and anti-CD4 (clone: GK1.5; BioXCell) mAbs starting one day before sensitization (day -1) and on day 3 and 6. This treatment routinely depleted >98% of target cells. To block CXCR3, mice were given i.p injections of 0.2 mg of anti-CXCR3 (clone: CXCR3-173; BioXCell) on day 6 and 9.

Preparation of ear cells

The ears were minced into small pieces and were incubated for 2 hours at 37°C in 10 ml digestion solution. The digestion solution is Iscove's Modified Dulbecco's Medium (Gibco, Grand Island, NY) containing collagenase D (1 mg/ml; Roche, Mannheim, Germany) and DNase I (0.1 mg/ml Roche, Mannheim, Germany). Digested ears were disrupted using Fisherbrand 150 handheld homogenizer, and cells were passed through a 70μm cell strainer (Falcon, Durham, USA). After erythrocytes removal using ACK Lysis Buffer (Gibco), cells were resuspended in PBS. Total viable cell numbers were determined by means of trypan blue exclusion.

Flow cytometric analysis

Ear cells were preincubated with truStain FcX anti-mouse CD16/32 mAb for 10 min at 4°C. The following antibodies were used in the analysis: APC-anti-mouse CD4 (clone: RM4-5), BV421-anti-mouse CD8 (clone: 53-6.7), BV421-anti-mouse PD-1 (clone: 29F.1A12), rat-anti-mouse CD11b-APC (clone: M1/70), FITC-anti-mouse CD45 (clone: 30-F11), BV711-anti-mouse CD11c (clone: N418), PE-anti-mouse F4/80 (clone: BM8) and APC-anti-mouse NK1.1 (clone:PK136). All the antibodies were from BioLegend (San Diego, CA). All FACS analyses were performed on LSRFortessa flow cytometer (BD Biosciences, San Jose, CA), and data were analyzed by using FlowJo software (Treestar, Ashland, TN).

Tissue Histology

Ear samples were collected on day 13 and fixed in 10% formalin-PBS. Tissue samples were processed and proceeded for hematoxylin-eosin staining by Applied Medical Research Laboratory (Osaka, Japan).

Adoptive T cell transfer

Wild-type and PD-$1^{-/-}$ C57BL/6 mice were sensitized with oxazolone as described above, and the inguinal lymph node and spleen were isolated after 7 days. The mixture of lymph node and spleen cells were labeled with FITC-anti-CD4 or FITC-anti-CD8 mAbs (Biolegend) and subsequently with anti-FITC microbeads (Miltenyi Biotec, Auburn, CA). $CD4^+$ and $CD8^+$ T cells were purified using AutoMACS (Miltenyi Biotec). A mixture of $7x10^6$ $CD4^+$ and $5x10^6$ $CD8^+$ T cells were injected intravenously into RAG$2^{-/-}$ mice. The recipient mice received a challenge with 0.2mg oxazolone immediately after T cell transfer.

Oxazolone-specific T-cell responses

Wild-type mice were sensitized with oxazolone, and the inguinal lymph nodes were obtained after 7 days. The isolated lymph node cells ($6x10^5$ cells) were tested for their capacity to produce IFN-γ in response to 0.1 mg/ml oxazolone. After 5 days of culture in a 96-well flat-bottomed plate, IFN-γ levels in the supernatant were determined by ELISA (R&D Systems, Minneapolis, MN). Oxazolone-specific IFN-γ production was calculated by subtracting the spontaneous cytokine release.

RNA Isolation and qPCR

Ear samples were stored in 0.6 ml RNAlater (Qiagen, Germantown, MD). Tissues were cut into small pieces, disrupted using a homogenizer and were passed through a 70-μm cell strainer. After washing twice with PBS, RNA was extracted using RNeasy Mini Kit (Qiagen). The extracted RNA was reverse transcribed to cDNA using the PrimeScript II kit (Takara-bio, Kusatsu, Japan) according to the manufacturer's instruction. Real-time PCR was performed with SSo Advanced Universal SYBR Green Supermix (Bio-Rad, Hercules, CA) using the CFX Connect Real-Time PCR Detection System (Bio-Rad). PCR was performed by an initial denaturation of 95 °C for 3 min, followed by 40 cycles of 95 °C for 15 s and 55 °C for 30 s. SYBR green fluorescence was measured at the end of each extension step. Melting curve analysis was performed to check the specificity of the PCR products. All samples were run in duplicate and averaged after normalization using β-actin as a housekeeping gene. Relative expression was quantified using $2^{-\Delta\Delta CT}$ calculation. Primer sequences were as follows: 5-TCTGCCATGAAGTCCGCTG -3 and 5- CAGGAGCATCGTGCATTCCT-3 for CXCL9; 5-GCCGTCATTTTCTGCCTCAT-3 and 5- GCTTCCCTATGGCCCTCATT-3 for CXCL10; 5- TTCACCACACTAAGGGGCTA -3 and 5- GCCACAGAGAGATGGTGTTC -3 for CCL19; and 5- ACTATTGGCAACGAGCGGTTC -3 and 5-GGATGCCACAGGATTCCATAC -3 for β-actin. To discriminate mRNA expression in $CD45^+$ and $CD45^-$ populations, ear cell suspension was labeled with FITC-anti-mouse CD45

mAb and anti-FITC microbeads as described above. $CD45^+$ and $CD45^-$ fractions were purified using AutoMACS by positive and negative selection, respectively.

Statistical analysis

Data represent mean ± SD. Statistical calculations were performed using Student's t-test (comparison between 2 groups) or Tukey-Kramer test (more than 2 groups). Statistical significance was accepted for p values less than 0.05.

Results

T cell-dependent exacerbation of CHS by anti-PD-L1 mAb treatment

Negative immunoregulation by PD-1 is so crucial to the immune system that its deficiency strongly augments inflammatory responses (Okazaki et al., 2013). We induced CHS in $PD\text{-}1^{-/-}$ mice and compared the intensity with wild-type mice. To induce CHS, we first sensitized mice with oxazolone at the abdominal skin and challenged at the ear with the same hapten 7 days later (Fig. 1A). The challenge with oxazolone was repeated every other day for 3 times. The extent of ear swelling was always greater in $PD\text{-}1^{-/-}$ mice than in wild-type mice after each challenge (Fig. 1B). We analyzed cell infiltrates in the ears two days after the third challenge and found an increase in $CD8^+$ T cell accumulation in $PD\text{-}1^{-/-}$ mice compared to wild-type mice (Fig. 1C).

PD-L1 blockade in wild-type mice reproduced the same trend. Treatment with anti-PD-L1 mAb significantly enhanced ear swelling as well as the remarkable increase of $CD8^+$ T cell accumulation in the ears (Fig. 1D, E). $CD4^+$ T cells in the ear tissue showed an increasing trend, though the difference was not significant. Histochemical examination of the affected ears confirmed massive infiltration of inflammatory cells in anti-PD-L1 mAb-treated mice (Fig. 1F). Time-course of ear swelling after a single challenge showed that it is peaking after 2 days and slowly regressed thereafter before it reached a constant level on day 10 (Fig. 1G). Inactivation of PD-1-dependent immunoregulation not only enhanced the intensity of swelling but also prolonged the peak levels for several more days.

CHS is generally recognized as a hapten-specific T cell-dependent inflammation, but T cell responses do not fully account for the inflammation in CHS. CHS in $RAG2^{-/-}$ mice induced a significant but lesser degree of ear swelling than in wild-type mice (Fig. 2A). Depletion of either $CD4^+$ or $CD8^+$ T cells had a moderate impact on CHS induction, but when both $CD4^+$ and $CD8^+$ T cells were depleted, ear swelling was greatly reduced to the levels observed in $RAG2^{-/-}$ mice (Fig. 2B). Although these results support T cell-dependence of CHS induction, ear swelling was still significant in the absence of T cells. It is consistent with previous papers regarding significant ear swelling by the CHS induction in $RAG2^{-/-}$ mice. This CHS-like response in $RAG2^{-/-}$ was mediated by NK cells in a hapten-specific manner (O'Leary et al., 2006; Rouzaire et al., 2012). Therefore, the blockade of PD-L1 might have exaggerated CHS by affecting T cell-dependent immune response and/or proinflammatory activities by innate immune cells.

PD-1 expression was originally discovered in activated T cells and B cells; however, more recently, NK cells and myeloid cells were also shown to express PD-1 (Krempski et al., 2011; Terme et al., 2012; Karyampudi et al., 2016; Gordon et al., 2017; Pesce et al., 2017; Hsu et al., 2018). In our CHS induction, PD-1 expression could be found not only in T cells

but also in NK cells and dendritic cells (Fig. 2C). While PD-1 blockade is known to enhance T cell immunity, anti-PD-L1 mAb treatment might have found different targets outside T cells. To examine this possibility, we applied anti-PD-L1 mAb to CHS induction in $RAG2^{-/-}$ mice. However, PD-L1 blockade did not enhance the ear swelling in $RAG2^{-/-}$ mice at all even after the extended 5-times challenges with oxazolone (Fig. 2D).

Before ear-infiltrated T cells exert the proinflammatory activities, they need to interact with antigen-presenting cells for recognition of the hapten. It was still possible that PD-L1 blockade had somehow substantially changed T cell-stimulatory functions of PD-1-expressing antigen-presenting cells. Previous experiment with $RAG2^{-/-}$ mice could not address such an indirect effect because they were lacking T cells. To test the significance of PD-1-expressing non-T cells in the presence of T cells, we injected $PD\text{-}1^{+/+}$ or $PD\text{-}1^{-/-}$ T cells to RAG2-KO mice and compared effects of anti-PD-L1 mAb on CHS. When $PD\text{-}1^{-/-}$ T cells were used, PD-L1 blockade would not provide a direct benefit on T cells, but $RAG2^{-/-}$ mice-derived non-T cells should be able to express PD-1. $PD\text{-}1^{-/-}$ T cell transfer certainly promoted ear swelling on top of the innate response in $RAG2^{-/-}$ mice, but anti-PD-L1 mAb failed to enhance CHS in this setting (Fig. 3A, B). Transfer of $PD\text{-}1^{+/+}$ T cells confirmed that anti-PD-L1 mAb is acting on T cells as observed in the further enhancement of ear swelling and $CD8^+$ T cell number (Fig. 3C, D). These results suggest that T cells are the primary target of CHS enhancement by anti-PD-L1 mAb. Although biological significance of PD-1 has been reported in NK cells and antigen-presenting cells (Krempski et al., 2011; Terme et al., 2012; Karyampudi et al., 2016; Gordon et al., 2017; Pesce et al., 2017; Hsu et al., 2018), liberation of non-T cells from PD-1-dependent immunoregulation might have little contribution to the enhancement of CHS, if any.

PD-L1 blockade promotes the priming of hapten-reactive T cells

CHS induction in this animal model consists of two different phases. The first is the sensitization phase where hapten application on dorsal or abdominal skin establishes hapten-reactive T cells. In the subsequent elicitation phase, a challenge with the same hapten at the ear recruits the hapten-reactive T cells and induce cutaneous inflammation. To examine which step is crucial to the immunopotentiation by PD-L1 blockade, we limited anti-PD-L1 mAb administration in either the sensitization phase or the elicitation phase. PD-L1 blockade only during the elicitation phase affected neither ear swelling nor T cell infiltration (Fig. 4A, B). In contrast, when PD-L1 blockade was provided during the sensitization phase but withheld in the elicitation phase, the treatment sufficiently enhanced ear swelling and $CD8^+$ T cell infiltration. Since PD-L1 blockade created a difference in the sensitization phase, we analyzed T cells in the inguinal lymph nodes after abdominal sensitization. T cell numbers in the lymph nodes did not significantly increase after the anti-PD-L1 mAb treatment (Fig. 4C). To examine hapten-specific T cell response, we restimulated the lymph node cells with oxazolone and found a significant increase of IFN-γ production in anti-PD-L1 mAb-treated mice (Fig. 4D). These results suggest that PD-L1 blockade could promote establishment of hapten-specific T cells in the sensitization, and the increase in hapten-specific T cells might be enough to enhance cutaneous inflammation.

Anti-PD-L1 mAb treatment in the sensitization phase alone promoted CHS, but interestingly, continuous PD-L1 blockade in both sensitization and elicitation phases further enhanced CHS (Fig. 4A, B). This increase indicates that anti-PD-L1 mAb could also enhance inflammatory responses in the elicitation phase. In agreement with this view, PD-L1 blockade enhanced the

elicitation phase of CHS in the transfer of effector T cells from oxazolone-sensitized mice to $RAG2^{-/-}$ mice (Fig. 3C, D).

PD-L1 blockade enhances CXCR3-dependent T cell accumulation

Treatment with anti-PD-L1 mAb increased numbers of inflammatory cells, especially $CD8^+$ T cells, in the affected ears. Chemokines such as CXCL9 and CXCL10 have been shown to recruit $CD8^+$ T cells to the inflamed tissues in disease models including allograft rejection and CHS (Melter et al., 2001; Dufour et al., 2002; Panzer et al., 2004). We examined whether these chemokines were responsible for the massive increase of $CD8^+$ T cells by PD-L1 blockade in CHS. Anti-PD-L1 mAb treatment upregulated CXCL9 and CXCL10 mRNA in the inflamed ears (Fig. 5A, B). mRNA levels of CCL19, which may attract dendritic cells and neutrophils via CCR7, did not increase by PD-L1 blockade (Fig. 5C). In the ear, $CD45^-$ cells of non-hematopoietic origin accounted for a large body of the chemokines induction by PD-L1 blockade (Fig. 5D). Such PD-L1 blockade-dependent increases were not observed in the $CD45^+$ fraction.

CXCR3 is a receptor for CXCL9 and CXCL10 and mediates immune cells recruitment to local inflamed sites. Blockade of CXCR3 significantly reduced ear swelling in the normal CHS induction and in the exaggerated CHS by anti-PD-L1 mAb (Fig. 5E). Corresponding to this change, $CD8^+$ T cell accumulation in the ear was largely decreased by anti-CXCR3 mAb treatment, confirming its central role in T cell recruitment to the local inflamed tissue (Fig. 5F). In contrast, local macrophage counts did not change by anti-PD-L1 mAb or anti-CXCR3 mAb (Fig. 5G). This experiment suggests that the pronounced CXCL9 and CXCL10 upregulation under PD-L1 blockade may be involved in the exaggerated cutaneous inflammation by promoting $CD8^+$ T cell accumulation.

PD-L1 blockade capitalizes on a suboptimal hapten exposure to induce significant dermatitis

The current study shows that distinct dermatitis in the hapten-induced CHS could be further exaggerated by the blockade of PD-1-dependent immunoregulation. However, irAE in PD-1 blockade therapy may be observed in tissues without previously recognizable inflammation. To reproduce this situation, we examined whether the immunopotentiation by anti-PD-L1 mAb was strong enough to escalate subtle inflammation to clearly visible dermatitis. We sought to determine a suboptimal dose of oxazolone and found that challenges with a dose as low as 20 μg did not demonstrate either significant tissue swelling or T cell accumulation in the ear (Fig. 6A-C). There was no escalation of ear swelling even after the repeated challenges at this dose. However, when combined with PD-L1 blockade, exposure to this dose of oxazolone resulted in notable dermatitis, which was intensified by the repeated challenge (Fig. 6D). Although a small number of T cells could be found in the ear with such a low dose of oxazolone, anti-PD-L1 mAb treatment increased $CD4^+$ and $CD8^+$ T cell numbers for 9- and 25-times (Fig. 6E). This result suggests that the enhancement of T cell immunity by the blockade of PD-1 pathway can transform unnoticeable skin irritation to significant dermatitis.

The analysis of chemokines expression showed that anti-PD-L1 mAb treatment upregulated mRNA levels of CXCL9 and CXCL10 in the ears challenged with 20 μg oxazolone (Fig. 6F). Anti-CXCR3 mAb downregulated ear swelling and T cell accumulation that were mostly caused by the anti-PD-L1 mAb treatment (Fig. 6G, H). PD-L1 blockade promoted $CD8^+$ T

cell-dominant immune responses in the local skin and thereby facilitated the emergence of significant dermatitis.

Discussion

PD-1-dependent immunoregulation plays a key role in cutaneous inflammation. In the current study, CHS induction in PD-$1^{-/-}$ mice using oxazolone significantly enhanced tissue swelling as well as $CD8^+$ T cell infiltration. Treatment of wild-type mice with anti-PD-L1 mAb also exaggerated dermatitis (Fig. 1) as it has been shown in CHS experiments using dinitrophenylfluorobenzene as a hapten (Tsushima et al., 2003; Gamradt et al., 2019).

Anti-PD-L1 mAb treatment during sensitization clearly increased oxazolone-reactive effector T cells in the draining lymph nodes (Fig. 4). This result indicates that the PD-1 signaling critically controls the development of antigen-specific effector T cells in the lymph nodes. Promoted expansion of oxazolone-specific T cells could sufficiently enhance subsequent induction of CHS, even though anti-PD-L1 mAb treatment was withheld during the elicitation phase. PD-1-dependent immunoregulation was also crucial in the elicitation phase because extended treatment with anti-PD-L1 mAb into the elicitation phase further enhanced CHS (Fig. 4). The enhancement of the elicitation phase by PD-L1 blockade was also evidenced from the T cell transfer experiment where the recipient mice received oxazolone challenge soon after the transfer of effector T cells from sensitized mice (Fig. 3C, D). Consistent with these findings, PD-1-dependent immunoregulation has been shown to be vital in the elicitation phase of T cell-dependent cutaneous inflammation. PD-L1 expression in keratinocytes can reduce the intensity of skin inflammation (Ritprajak et al., 2010; Okiyama and Katz, 2014). Hapten-specific effector T cells are prone to PD-1-mediated inactivation since transfer of PD-L1-expressing dendritic cells to the sensitized mice downregulated CHS (Kim et al., 2006). CHS induction establishes tissue-resident $CD8^+$ T cells in the skin, and PD-1 blockade in rechallenge augmented recall response of tissue-resident T cells in the enhanced dermatitis (Gamradt et al., 2019).

Interestingly, PD-1 blockade was previously reported to have no effect on CHS when applied only in the elicitation phase (Tsushima et al., 2003). Our data also showed no enhancement of inflammation when treatment with anti-PD-L1 mAb started 7 days after the sensitization (Fig. 4). It is unclear why the treatment in the elicitation phase alone failed to enhance the inflammation, but it may be related to the numbers of hapten-reactive T cells. In the draining lymph nodes of sensitized mice without PD-L1 blockade, IFN-γ production in response to oxazolone was very little (Fig. 4). Possibly, the number of oxazolone-reactive T cells after the conventional sensitization might be so small that immunopotentiation by PD-L1 blockade could not produce a significant impact in the subsequent elicitation phase. However, PD-1/PD-L1 blockade during the elicitation phase may significantly enhance the inflammation when a large number of hapten-specific effector T cells is available, e.g. vigorous induction with a help from PD-L1 blockade in the sensitization (Fig. 4) or effector T cell transfer into RAG$2^{-/-}$ recipients (Fig. 3). Multiple episodes of antigen exposure may enhance antigen-specific T cell immunity to the above threshold levels. Patients with such a history may be vulnerable to the emergence of irAE by PD-1/PD-L1 blockade.

The importance of T cells, especially $CD8^+$ T cells, in CHS has been demonstrated in previous reports (Gocinski and Tigelaar, 1990; Bour et al., 1995; Akiba et al., 2002; He et al., 2009). In our experiment, depletion of $CD4^+$ and $CD8^+$ T cells from wild-type mice inhibited

CHS induction and reduced ear swelling to the levels equivalent to those observed in RAG2$^{-/-}$ mice (Fig. 2). Although T cells are important players in CHS, the considerable ear swelling in the absence of T cells (Fig. 2) indicates that non-T cells play a direct role in the cutaneous inflammation (Honda et al., 2013). In the original report on NK cell memory, CHS induction in RAG2$^{-/-}$ mice demonstrated significant ear swelling in an antigen (hapten)-specific manner (O'Leary et al., 2006). Their study showed that NK cells were responsible for the cutaneous inflammation in RAG2$^{-/-}$ mice because NK cell depletion abolished the ear swelling. This NK cell-dependent CHS involves unconventional ear inflammation with fewer cell infiltrates (Rouzaire et al., 2012). Similar to the fellow lymphocytes, NK cells can express PD-1 after activation, and interaction of their PD-1 with PD-L1 downregulates NK activities (Terme et al., 2012; Pesce et al., 2017; Hsu et al., 2018). The significance of PD-1 in monocytes remains unclear, but it may be related to M2-type functions, and their anti-inflammatory nature may contribute to the immunosuppressive tumor microenvironment (Gordon et al., 2017; Strauss et al., 2020). Along with T cells, these cell types were found to express PD-1 in the hapten-challenged ear (Fig. 2). PD-L1 blockade on myeloid lineage or NK cells did not affect the intensity of dermatitis (Fig. 2). The results from T cell transfer experiment excluded the possibility that PD-1-expressing non-T cells might indirectly exaggerate the inflammation by promoting T cell activity (Fig. 3). These results strongly suggest that PD-1-expressing T cells, but not myeloid lineage or NK cells, are the predominant target of anti-PD-L1 mAb treatment in the enhancement of dermatitis.

Correlated with the remarkable increase of ear-infiltrated CD8^{+} T cells, PD-L1 blockade upregulated CXCL9 and CXCL10 (Fig. 4). These chemokines are responsible for CD8^{+} T cell recruitment in various inflammation models (Melter et al., 2001; Dufour et al., 2002; Panzer et al., 2004) and in tumors (Chamoto et al., 2017; Chow et al., 2019). CXCL9 and CXCL10 are induced in the normal course of CHS in mice (Tokuriki et al., 2002; Mitsui et al., 2003; He et al., 2009) and humans (Goebeler et al., 2001), and their blockade can reduce CHS intensity (Nakae et al., 2003; He et al., 2009). CXCL9 and CXCL10 recruit T cells via CXCR3. Blockade of CXCR3 reduced T cell infiltration and attenuated ear swelling in anti-PD-L1 mAb-treated mice (Fig. 5). Such a role of the CXCR3 chemokine system is consistent with tumor studies in which vigorous anti-tumor activities of CD8^{+} T cell response by the PD-1 blockade accompanies CXCL9/10 upregulation. CXCR3 blockade abolished intratumoral CD8^{+} T cell infiltration and anti-tumor efficacy of the PD-1 blockade therapy (Chamoto et al., 2017; Chow et al., 2019). While anti-PD-L1 mAb targets T cells in the enhancement of CHS (Figs. 2, 3), significant upregulation of CXCL9 and CXCL10 were observed in CD45^{-} cells (Fig. 5). The chemokine-producing non-hematopoietic cells might be keratinocytes, which has been shown to produce CXCL9 and CXCL10 in CHS (Albanesi et al., 2000; Mahalingam et al., 2001; Sebastiani et al., 2002). It is possible that PD-L1 blockade enhanced IFN-γ production from activated T cells, and thereby keratinocytes upregulated these IFN-γ-inducible chemokines (Tokuriki et al., 2002; Mori et al., 2008).

The exaggeration of CHS in this study and tumor regression in the immune checkpoint therapy are both initiated by the inactivation of PD-1 pathway; therefore, it is not surprising to find some similarities in between. As discussed above, the activation of CD8^{+} T cell-dominant immune response is important in both cases, and those T cells were recruited by CXCR3-chemokines. Another example is the promotion of antigen-specific T cell development as the mechanism of action. PD-L1 blockade during the sensitization with oxazolone promoted the induction of hapten-reactive T cells in the draining lymph nodes, and this increase was significant enough to enhance subsequent dermatitis induction (Fig. 4). Correspondingly, surgical removal of tumor-draining lymph node abolished anti-tumor

efficacy of anti-PD-L1 mAb (Chamoto et al., 2017). This finding indicates that the enhancement of effector functions of pre-existing tumor-infiltrated T cells might be insufficient but priming of anti-tumor effector T cells in the lymph nodes is crucial to achieve tumor regression by PD-1 blockade.

Experimental CHS induction in the presence of anti-PD-L1 mAb also shares an inflammatory profile with human irAE in the skin. Skin tissues of cancer patients who received PD-1 blockade therapy demonstrated notable $CD8^+$ T cell infiltration and apoptotic keratinocytes. The increase of perforin, granzyme B, CXCL9 and CXCL10 suggested proinflammatory activities of these $CD8^+$ T cells in the skin. Gene expression profile in the skin from subjects of PD-1 blockade therapy resembled that of immune-related skin diseases such as acute GVHD and toxic epidermal necrolysis (Goldinger et al., 2016). Indeed, although most skin problems related to PD-1/PD-L1-blocking agents are mild, those agents are reported to rarely induce severe irAE such as Stevens-Johnson syndrome and toxic epidermal necrolysis (Saw et al., 2017; Haratake et al., 2018; Salati et al., 2018; Coleman et al., 2020; Robinson et al., 2020). Clinically, occurrence of irAE may be associated with anti-tumor efficacy of PD-1 blockade therapy. Improvement of progression-free survival has been reported in patients who experienced irAE including dermatological inflammation (Hua et al., 2016; Rogado et al., 2019; Khan et al., 2020). This correlation seems to be reasonable because the same type of immune responses may be responsible for tumor regression and irAE induction as a result of PD-1/PD-L1 blockade.

Dermal irAE may arise in the previously asymptomatic skin as a result of immune checkpoint blockade therapy. Interestingly, minimum levels of skin irritation by a low dose of oxazolone were exaggerated to clearly visible dermatitis, suggesting that the proinflammatory effect of PD-L1 blockade had a great influence on dermatitis (Fig. 6). Compared to the high dose setting, which represents pre-existing significant inflammatory conditions, this suboptimal setting may be closer to the clinical situation. Since a low dose of oxazolone alone hardly induced dermatitis (Fig. 6), dermatitis in this setting was essentially caused by the proinflammatory effect of PD-L1 blockade. Although CHS is resulted from combined proinflammatory responses by T cells and innate immune cells, we have shown here that anti-PD-L1 mAb treatment predominantly promotes T cell-dependent immune response (Figs. 2, 3). Fold increase of accumulated T cell numbers were pronounced in the low-dose setting, suggesting that dermatitis caused by PD-1/PD-L1 blockade might involve more substantial contribution from T cell-dependent inflammation than the same levels of inflammation by conventional CHS induction. Therefore, dermatitis induction as the result of PD-1/PD-L1 blockade, i.e. dermal irAE, may be a relatively T cell-predominant form of inflammation.

In conclusion, the blockade of PD-1 signaling exaggerated CHS with massive $CD8^+$ T cell infiltration. The mechanism involves the enhancement of antigen-specific T cell development and their accumulation into the local skin tissue through upregulation of CXCL9 and CXCL10. These changes in the CHS enhancement by PD-1 blockade shares features with clinical observations in dermal irAE, which shows $CD8^+$ T cell-dominant form of cutaneous inflammation. Our experiment with a low dose of oxazolone indicates that the blockade of PD-1 pathway could substantiate a predisposing stealthy inflammation to prominent dermatitis. This experimental approach may be useful in the analysis of dermal irAE and in developing treatment for this inflammatory complication.

Conflict of Interest

The authors declare that the research was conducted in the absence of any commercial or financial relationships that could be construed as a potential conflict of interest.

Author contributions

TH and AO designed the study. MA, KS, YT and MT performed the experiments and analyzed the data with AO. NI performed statistical analyses. AO wrote the first draft of the manuscript. MA contributed sections of the manuscript. All authors contributed to and approved the manuscript.

Acknowledgements

The authors would like to thank to Miwa Okada, Kumiko Yonezaki and Yukako Kamita for technical support and maintenance of mice colonies. The authors are thankful to Dr. Kenji Chamoto for reading and providing feedback on the manuscript.

References

Akiba, H., Kehren, J., Ducluzeau, M.T., Krasteva, M., Horand, F., Kaiserlian, D., et al. (2002). Skin inflammation during contact hypersensitivity is mediated by early recruitment of CD8+ T cytotoxic 1 cells inducing keratinocyte apoptosis. *J Immunol* 168(6)**,** 3079-3087. doi: 10.4049/jimmunol.168.6.3079.

Albanesi, C., Scarponi, C., Sebastiani, S., Cavani, A., Federici, M., De Pità, O., et al. (2000). IL-4 enhances keratinocyte expression of CXCR3 agonistic chemokines. *J Immunol* 165(3)**,** 1395-1402. doi: 10.4049/jimmunol.165.3.1395.

Bour, H., Peyron, E., Gaucherand, M., Garrigue, J.L., Desvignes, C., Kaiserlian, D., et al. (1995). Major histocompatibility complex class I-restricted CD8+ T cells and class II-restricted CD4+ T cells, respectively, mediate and regulate contact sensitivity to dinitrofluorobenzene. *Eur J Immunol* 25(11)**,** 3006-3010. doi: 10.1002/eji.1830251103.

Chamoto, K., Chowdhury, P.S., Kumar, A., Sonomura, K., Matsuda, F., Fagarasan, S., et al. (2017). Mitochondrial activation chemicals synergize with surface receptor PD-1 blockade for T cell-dependent antitumor activity. *Proc Natl Acad Sci U S A* 114(5)**,** E761-E770. doi: 10.1073/pnas.1620433114.

Chamoto, K., Hatae, R., and Honjo, T. (2020). Current issues and perspectives in PD-1 blockade cancer immunotherapy. *Int J Clin Oncol* 25(5)**,** 790-800. doi: 10.1007/s10147-019-01588-7.

Chow, M.T., Ozga, A.J., Servis, R.L., Frederick, D.T., Lo, J.A., Fisher, D.E., et al. (2019). Intratumoral Activity of the CXCR3 Chemokine System Is Required for the Efficacy of Anti-PD-1 Therapy. *Immunity* 50(6)**,** 1498-1512 e1495. doi: 10.1016/j.immuni.2019.04.010.

Coleman, E.L., Olamiju, B., and Leventhal, J.S. (2020). The life-threatening eruptions of immune checkpoint inhibitor therapy. *Clin Dermatol* 38(1)**,** 94-104. doi: 10.1016/j.clindermatol.2019.10.015.

Dufour, J.H., Dziejman, M., Liu, M.T., Leung, J.H., Lane, T.E., and Luster, A.D. (2002). IFN-gamma-inducible protein 10 (IP-10; CXCL10)-deficient mice reveal a role for IP-10 in effector T cell generation and trafficking. *J Immunol* 168(7)**,** 3195-3204. doi: 10.4049/jimmunol.168.7.3195.

Gamradt, P., Laoubi, L., Nosbaum, A., Mutez, V., Lenief, V., Grande, S., et al. (2019). Inhibitory checkpoint receptors control CD8(+) resident memory T cells to prevent skin allergy. *J Allergy Clin Immunol* 143(6)**,** 2147-2157 e2149. doi: 10.1016/j.jaci.2018.11.048.

Gocinski, B.L., and Tigelaar, R.E. (1990). Roles of CD4+ and CD8+ T cells in murine contact sensitivity revealed by in vivo monoclonal antibody depletion. *J Immunol* 144(11)**,** 4121-4128.

Goebeler, M., Trautmann, A., Voss, A., Bröcker, E.V., Toksoy, A., and Gillitzer, R. (2001). Differential and sequential expression of multiple chemokines during elicitation of allergic contact hypersensitivity. *Am J Pathol* 158(2)**,** 431-440. doi: 10.1016/s0002-9440(10)63986-7.

Goldinger, S.M., Stieger, P., Meier, B., Micaletto, S., Contassot, E., French, L.E., et al. (2016). Cytotoxic Cutaneous Adverse Drug Reactions during Anti-PD-1 Therapy. *Clin Cancer Res* 22(16)**,** 4023-4029. doi: 10.1158/1078-0432.ccr-15-2872.

Gordon, S.R., Maute, R.L., Dulken, B.W., Hutter, G., George, B.M., McCracken, M.N., et al. (2017). PD-1 expression by tumour-associated macrophages inhibits phagocytosis and tumour immunity. *Nature* 545(7655)**,** 495-499. doi: 10.1038/nature22396.

Haratake, N., Tagawa, T., Hirai, F., Toyokawa, G., Miyazaki, R., and Maehara, Y. (2018). Stevens-Johnson Syndrome Induced by Pembrolizumab in a Lung Cancer Patient. *J Thorac Oncol* 13(11)**,** 1798-1799. doi: 10.1016/j.jtho.2018.05.031.

He, D., Wu, L., Kim, H.K., Li, H., Elmets, C.A., and Xu, H. (2009). IL-17 and IFN-gamma mediate the elicitation of contact hypersensitivity responses by different mechanisms and both are required for optimal responses. *J Immunol* 183(2)**,** 1463-1470. doi: 10.4049/jimmunol.0804108.

Honda, T., Egawa, G., Grabbe, S., and Kabashima, K. (2013). Update of immune events in the murine contact hypersensitivity model: toward the understanding of allergic contact dermatitis. *J Invest Dermatol* 133(2)**,** 303-315. doi: 10.1038/jid.2012.284.

Hsu, J., Hodgins, J.J., Marathe, M., Nicolai, C.J., Bourgeois-Daigneault, M.C., Trevino, T.N., et al. (2018). Contribution of NK cells to immunotherapy mediated by PD-1/PD-L1 blockade. *J Clin Invest* 128(10)**,** 4654-4668. doi: 10.1172/jci99317.

Hua, C., Boussemart, L., Mateus, C., Routier, E., Boutros, C., Cazenave, H., et al. (2016). Association of Vitiligo With Tumor Response in Patients With Metastatic Melanoma Treated With Pembrolizumab. *JAMA Dermatol* 152(1)**,** 45-51. doi: 10.1001/jamadermatol.2015.2707.

Iwai, Y., Ishida, M., Tanaka, Y., Okazaki, T., Honjo, T., and Minato, N. (2002). Involvement of PD-L1 on tumor cells in the escape from host immune system and tumor immunotherapy by PD-L1 blockade. *Proc Natl Acad Sci U S A* 99(19)**,** 12293-12297. doi: 10.1073/pnas.192461099.

Karyampudi, L., Lamichhane, P., Krempski, J., Kalli, K.R., Behrens, M.D., Vargas, D.M., et al. (2016). PD-1 Blunts the Function of Ovarian Tumor-Infiltrating Dendritic Cells by Inactivating NF-κB. *Cancer Res* 76(2)**,** 239-250. doi: 10.1158/0008-5472.can-15-0748.

Khan, Z., Di Nucci, F., Kwan, A., Hammer, C., Mariathasan, S., Rouilly, V., et al. (2020). Polygenic risk for skin autoimmunity impacts immune checkpoint blockade in bladder cancer. *Proc Natl Acad Sci U S A* 117(22)**,** 12288-12294. doi: 10.1073/pnas.1922867117.

Kim, H.K., Guan, H., Zu, G., Li, H., Wu, L., Feng, X., et al. (2006). High-level expression of B7-H1 molecules by dendritic cells suppresses the function of activated T cells and desensitizes allergen-primed animals. *J Leukoc Biol* 79(4)**,** 686-695. doi: 10.1189/jlb.0805436.

Krempski, J., Karyampudi, L., Behrens, M.D., Erskine, C.L., Hartmann, L., Dong, H., et al. (2011). Tumor-infiltrating programmed death receptor-1+ dendritic cells mediate immune suppression in ovarian cancer. *J Immunol* 186(12)**,** 6905-6913. doi: 10.4049/jimmunol.1100274.

Mahalingam, S., Chaudhri, G., Tan, C.L., John, A., Foster, P.S., and Karupiah, G. (2001). Transcription of the interferon gamma (IFN-gamma)-inducible chemokine Mig in IFN-gamma-deficient mice. *J Biol Chem* 276(10)**,** 7568-7574. doi: 10.1074/jbc.M005773200.

Melter, M., Exeni, A., Reinders, M.E., Fang, J.C., McMahon, G., Ganz, P., et al. (2001). Expression of the chemokine receptor CXCR3 and its ligand IP-10 during human cardiac allograft rejection. *Circulation* 104(21)**,** 2558-2564. doi: 10.1161/hc4601.098010.

Michot, J.M., Bigenwald, C., Champiat, S., Collins, M., Carbonnel, F., Postel-Vinay, S., et al. (2016). Immune-related adverse events with immune checkpoint blockade: a comprehensive review. *Eur J Cancer* 54**,** 139-148. doi: 10.1016/j.ejca.2015.11.016.

Mitsui, G., Mitsui, K., Hirano, T., Ohara, O., Kato, M., and Niwano, Y. (2003). Kinetic profiles of sequential gene expressions for chemokines in mice with contact hypersensitivity. *Immunol Lett* 86(2)**,** 191-197. doi: 10.1016/s0165-2478(03)00017-8.

Mori, T., Kabashima, K., Yoshiki, R., Sugita, K., Shiraishi, N., Onoue, A., et al. (2008). Cutaneous hypersensitivities to hapten are controlled by IFN-gamma-upregulated keratinocyte Th1 chemokines and IFN-gamma-downregulated langerhans cell Th2 chemokines. *J Invest Dermatol* 128(7)**,** 1719-1727. doi: 10.1038/jid.2008.5.

Nakae, S., Komiyama, Y., Narumi, S., Sudo, K., Horai, R., Tagawa, Y., et al. (2003). IL-1-induced tumor necrosis factor-alpha elicits inflammatory cell infiltration in the skin by inducing IFN-gamma-inducible protein 10 in the elicitation phase of the contact hypersensitivity response. *Int Immunol* 15(2)**,** 251-260. doi: 10.1093/intimm/dxg028.

Nishimura, H., Nose, M., Hiai, H., Minato, N., and Honjo, T. (1999). Development of lupus-like autoimmune diseases by disruption of the PD-1 gene encoding an ITIM motif-carrying immunoreceptor. *Immunity* 11(2)**,** 141-151. doi: 10.1016/s1074-7613(00)80089-8.

Nishimura, H., Okazaki, T., Tanaka, Y., Nakatani, K., Hara, M., Matsumori, A., et al. (2001). Autoimmune dilated cardiomyopathy in PD-1 receptor-deficient mice. *Science* 291(5502)**,** 319-322. doi: 10.1126/science.291.5502.319.

O'Leary, J.G., Goodarzi, M., Drayton, D.L., and von Andrian, U.H. (2006). T cell- and B cell-independent adaptive immunity mediated by natural killer cells. *Nat Immunol* 7(5)**,** 507-516. doi: 10.1038/ni1332.

Okazaki, T., Chikuma, S., Iwai, Y., Fagarasan, S., and Honjo, T. (2013). A rheostat for immune responses: the unique properties of PD-1 and their advantages for clinical application. *Nat Immunol* 14(12)**,** 1212-1218. doi: 10.1038/ni.2762.

Okiyama, N., and Katz, S.I. (2014). Programmed cell death 1 (PD-1) regulates the effector function of CD8 T cells via PD-L1 expressed on target keratinocytes. *J Autoimmun* 53**,** 1-9. doi: 10.1016/j.jaut.2014.06.005.

Panzer, U., Reinking, R.R., Steinmetz, O.M., Zahner, G., Sudbeck, U., Fehr, S., et al. (2004). CXCR3 and CCR5 positive T-cell recruitment in acute human renal allograft rejection. *Transplantation* 78(9)**,** 1341-1350. doi: 10.1097/01.tp.0000140483.59664.64.

Pesce, S., Greppi, M., Tabellini, G., Rampinelli, F., Parolini, S., Olive, D., et al. (2017). Identification of a subset of human natural killer cells expressing high levels of programmed death 1: A phenotypic and functional characterization. *J Allergy Clin Immunol* 139(1)**,** 335-346 e333. doi: 10.1016/j.jaci.2016.04.025.

Ritprajak, P., Hashiguchi, M., Tsushima, F., Chalermsarp, N., and Azuma, M. (2010). Keratinocyte-associated B7-H1 directly regulates cutaneous effector CD8+ T cell responses. *J Immunol* 184(9)**,** 4918-4925. doi: 10.4049/jimmunol.0902478.

Robinson, S., Saleh, J., Curry, J.L., and Mudaliar, K. (2020). Pembrolizumab-Induced Stevens-Johnson Syndrome/Toxic Epidermal Necrolysis in a Patient With Metastatic Cervical Squamous Cell Carcinoma: A Case Report. *Am J Dermatopathol* 42(4)**,** 292-296. doi: 10.1097/dad.0000000000001527.

Rogado, J., Sánchez-Torres, J.M., Romero-Laorden, N., Ballesteros, A.I., Pacheco-Barcia, V., Ramos-Leví, A., et al. (2019). Immune-related adverse events predict the therapeutic efficacy of anti-PD-1 antibodies in cancer patients. *Eur J Cancer* 109**,** 21-27. doi: 10.1016/j.ejca.2018.10.014.

Rouzaire, P., Luci, C., Blasco, E., Bienvenu, J., Walzer, T., Nicolas, J.F., et al. (2012). Natural killer cells and T cells induce different types of skin reactions during recall responses to haptens. *Eur J Immunol* 42(1)**,** 80-88. doi: 10.1002/eji.201141820.

Salati, M., Pifferi, M., Baldessari, C., Bertolini, F., Tomasello, C., Cascinu, S., et al. (2018). Stevens-Johnson syndrome during nivolumab treatment of NSCLC. *Ann Oncol* 29(1)**,** 283-284. doi: 10.1093/annonc/mdx640.

Sanmamed, M.F., and Chen, L. (2018). A Paradigm Shift in Cancer Immunotherapy: From Enhancement to Normalization. *Cell* 175(2)**,** 313-326. doi: 10.1016/j.cell.2018.09.035.

Saw, S., Lee, H.Y., and Ng, Q.S. (2017). Pembrolizumab-induced Stevens-Johnson syndrome in non-melanoma patients. *Eur J Cancer* 81**,** 237-239. doi: 10.1016/j.ejca.2017.03.026.

Sebastiani, S., Albanesi, C., De, P.O., Puddu, P., Cavani, A., and Girolomoni, G. (2002). The role of chemokines in allergic contact dermatitis. *Arch Dermatol Res* 293(11)**,** 552-559. doi: 10.1007/s00403-001-0276-9.

Strauss, L., Mahmoud, M.A.A., Weaver, J.D., Tijaro-Ovalle, N.M., Christofides, A., Wang, Q., et al. (2020). Targeted deletion of PD-1 in myeloid cells induces antitumor immunity. *Sci Immunol* 5(43). doi: 10.1126/sciimmunol.aay1863.

Terme, M., Ullrich, E., Aymeric, L., Meinhardt, K., Coudert, J.D., Desbois, M., et al. (2012). Cancer-induced immunosuppression: IL-18-elicited immunoablative NK cells. *Cancer Res* 72(11)**,** 2757-2767. doi: 10.1158/0008-5472.can-11-3379.

Tokuriki, A., Seo, N., Ito, T., Kumakiri, M., Takigawa, M., and Tokura, Y. (2002). Dominant expression of CXCR3 is associated with induced expression of IP-10 at hapten-challenged sites of murine contact hypersensitivity: a possible role for interferon-gamma-producing CD8(+) T cells in IP-10 expression. *J Dermatol Sci* 28(3)**,** 234-241. doi: 10.1016/s0923-1811(01)00172-4.

Topalian, S.L., Hodi, F.S., Brahmer, J.R., Gettinger, S.N., Smith, D.C., McDermott, D.F., et al. (2012). Safety, activity, and immune correlates of anti-PD-1 antibody in cancer. *N Engl J Med* 366(26)**,** 2443-2454. doi: 10.1056/NEJMoa1200690.

Tsushima, F., Iwai, H., Otsuki, N., Abe, M., Hirose, S., Yamazaki, T., et al. (2003). Preferential contribution of B7-H1 to programmed death-1-mediated regulation of hapten-specific allergic inflammatory responses. *Eur J Immunol* 33(10)**,** 2773-2782. doi: 10.1002/eji.200324084.

Wang, J., Okazaki, I.M., Yoshida, T., Chikuma, S., Kato, Y., Nakaki, F., et al. (2010). PD-1 deficiency results in the development of fatal myocarditis in MRL mice. *Int Immunol* 22(6)**,** 443-452. doi: 10.1093/intimm/dxq026.

Wang, J., Yoshida, T., Nakaki, F., Hiai, H., Okazaki, T., and Honjo, T. (2005). Establishment of NOD-Pdcd1-/- mice as an efficient animal model of type I diabetes. *Proc Natl Acad Sci U S A* 102(33)**,** 11823-11828. doi: 10.1073/pnas.0505497102.

Young, A., Quandt, Z., and Bluestone, J.A. (2018). The Balancing Act between Cancer Immunity and Autoimmunity in Response to Immunotherapy. *Cancer Immunol Res* 6(12)**,** 1445-1452. doi: 10.1158/2326-6066.cir-18-0487.

Figure legends

Figure 1. PD-1-dependent regulation of oxazolone-induced contact hypersensitivity. (A) Schedule of CHS induction. C57BL/6 mice were sensitized with oxazolone and received challenges at the ear on day 7, 9 and 11. Anti-PD-L1 mAb was given as indicated by black arrows. The extent of ear swelling is the ear thickness on day 9 (1st), 11 (2nd) and 13 (3rd) subtracted by the thickness before the challenge on day 7. (B, C) Challenges with oxazolone (200 μg) induced stronger skin inflammation in PD-$1^{-/-}$ mice than in wild-type mice as indicated by the extent of ear swelling (B) and $CD8^+$ T cell infiltration in the ears (C). (D-F) Treatment of wild-type mice with anti-PD-L1 mAb enhanced ear swelling (D) and $CD8^+$ T cell infiltration (E). Tissue histochemistry (F) confirmed accumulation of inflammatory cells in the ear after 3-times challenge with oxazolone and further enhancement by anti-PD-L1 mAb treatment. (G) Time-dependent changes in ear swelling after one-time challenge with oxazolone. Data represent average ± SD of 5 mice. b, $p < 0.01$; c, $p < 0.001$ vs corresponding control groups (Student's t-test).

Figure 2. T cells are the principal targets of CHS enhancement by PD-L1 blockade. (A) CHS induction with 200 μg oxazolone in RAG$2^{-/-}$ mice resulted in a significant but weaker ear swelling than wild-type mice. (B) T cell depletion in wild-type mice reduced the extent of CHS. Anti-CD4 and/or anti-CD8 mAbs were injected on day -1, 3 and 6. (C) PD-1 expression in the ear-infiltrated cells. Flow cytometric profiles indicate PD-1-positive percentage within $CD4^+$, $CD8^+$, $NK1.1^+$ and $CD11c^+$ population after gating for $CD45^+$ events. (D) Anti-PD-L1 mAb treatment did not exaggerate ear swelling in RAG$2^{-/-}$ mice. Data represent average ± SD of 5 mice. b, $p < 0.01$; c, $p < 0.001$ vs corresponding control groups (Student's t-test). *, $p < 0.05$; **, $p < 0.01$ vs no Ab group (Tukey-Kramer test).

Figure 3. Adoptive transfer of CHS effector T cells into RAG$2^{-/-}$ mice reconstituted immunopotentiation by anti-PD-L1 mAb. Effector T cells were obtained from oxazolone-sensitized wild-type (C, D) and PD-$1^{-/-}$ mice (A, B). Oxazolone dose for challenge was 200 μg. PD-L1 blockade enhanced ear swelling (A, C) and $CD8^+$ T cell accumulation (B, D) when effector T cells were from wild-type mice, but not PD-$1^{-/-}$ mice. Data represent average ± SD of 5 mice. a, $p < 0.05$; b, $p < 0.01$; c, $p < 0.001$ vs corresponding control groups (Student's t-test).

Figure 4. PD-L1 blockade could exaggerate CHS through the promotion of effector T cell development during sensitization. (A, B) Anti-PD-L1 mAb was given to the mice on either the sensitization phase (day 0 and 3) or the elicitation phase (day 7, 9, 11). Oxazolone dose for challenge was 200 μg. Ear swelling (A) and $CD8^+$ T cell accumulation (B) by PD-L1 blockade in the sensitization phase were further enhanced by the extended anti-PD-L1 mAb treatment in the elicitation phase. (C, D) PD-L1 blockade during sensitization promoted the establishment of hapten-reactive T cells. The inguinal lymph nodes were analyzed 7 days after the sensitization on the abdomen. T cell numbers (C) did not change, but anti-PD-L1 mAb treatment during sensitization notably increased IFN-γ production in response to ex vivo restimulation with oxazolone (0.1 mg/ml) for 5 days (D). Oxazolone-specific cytokine production was calculated as IFN-γ levels in the supernatant of oxazolone-stimulated lymph node cells subtracted by the levels in the unstimulated culture. Data represent average ± SD of 5 mice. Ex vivo restimulation of lymph mode cells were conducted in triplicate for each of 3 mice. b, $p < 0.01$ vs the control group (Student's t-test). *, $p < 0.05$; **, $p < 0.01$ between indicated groups (Tukey-Kramer test).

Figure 5. PD-L1 blockade enhanced $CD8^+$ T cell accumulation by upregulating CXCL9 and CXCL10 in the inflamed ear. (A-C) mRNA levels of chemokines in the ear 24h after the first challenge with oxazolone (200 μg). Anti-PD-L1 mAb treatment upregulated CXCL9 (A) and CXCL10 (B), but not CCL19 (C). (D) Upregulation of CXCL9 and CXCL10 was found in ear cells of non-hematopoietic origin ($CD45^-$). mRNA levels were determined by qPCR using 5 (A-C) or 3 mice (D) per group. (E-G) Blockade of CXCR3 reduced the extent of swelling (E) and $CD8^+$ T cell accumulation in the ear (F). Anti-CXCR3 mAb (dose) was given on day 6 and 9. Blockade of PD-L1 or CXCR3 did not affect $F4/80^+$ macrophages in the ear (G). Data represent average ± SD of 5 mice. a, $p < 0.05$; b, $p < 0.01$; c, $p < 0.001$ vs corresponding control groups. *, $p < 0.05$; **, $p < 0.01$ between indicated groups (Tukey-Kramer test).

Figure 6. Exposure to a low dose of oxazolone did not demonstrate significant signs of dermatitis, but anti-PD-L1 mAb triggered remarkable tissue inflammation. (A-C) Dose-dependent CHS induction by oxazolone. A dose as low as 20 μg did not induce significant ear swelling (A) and T cell accumulation (B, C) by repeated challenges. (D, E) Although oxazolone (20 μg) alone did not induce significant inflammation, its combination with anti-PD-L1 mAb caused notable swelling (D) and T cell accumulation (E) in the ear. (F) Anti-PD-L1 mAb treatment upregulated CXCL9 and CXCL10 mRNA in the ears 24h after the challenge with 20 μg oxazolone. Oxazolone alone did not change the chemokine mRNA levels compared to untreated controls. (G, H) Anti-CXCR3 mAb suppressed the induction of era swelling (G) and T cell accumulation (H) by the suboptimal exposure to oxazolone (20 μg) plus PD-L1 blockade. Data represent average ± SD of 3 (A-C) or 5 (D-H) mice. a, $p < 0.05$; b, $p < 0.01$; c, $p < 0.001$ vs corresponding control groups (Student's t-test). **, $p < 0.01$ between indicated groups (Tukey-Kramer test).

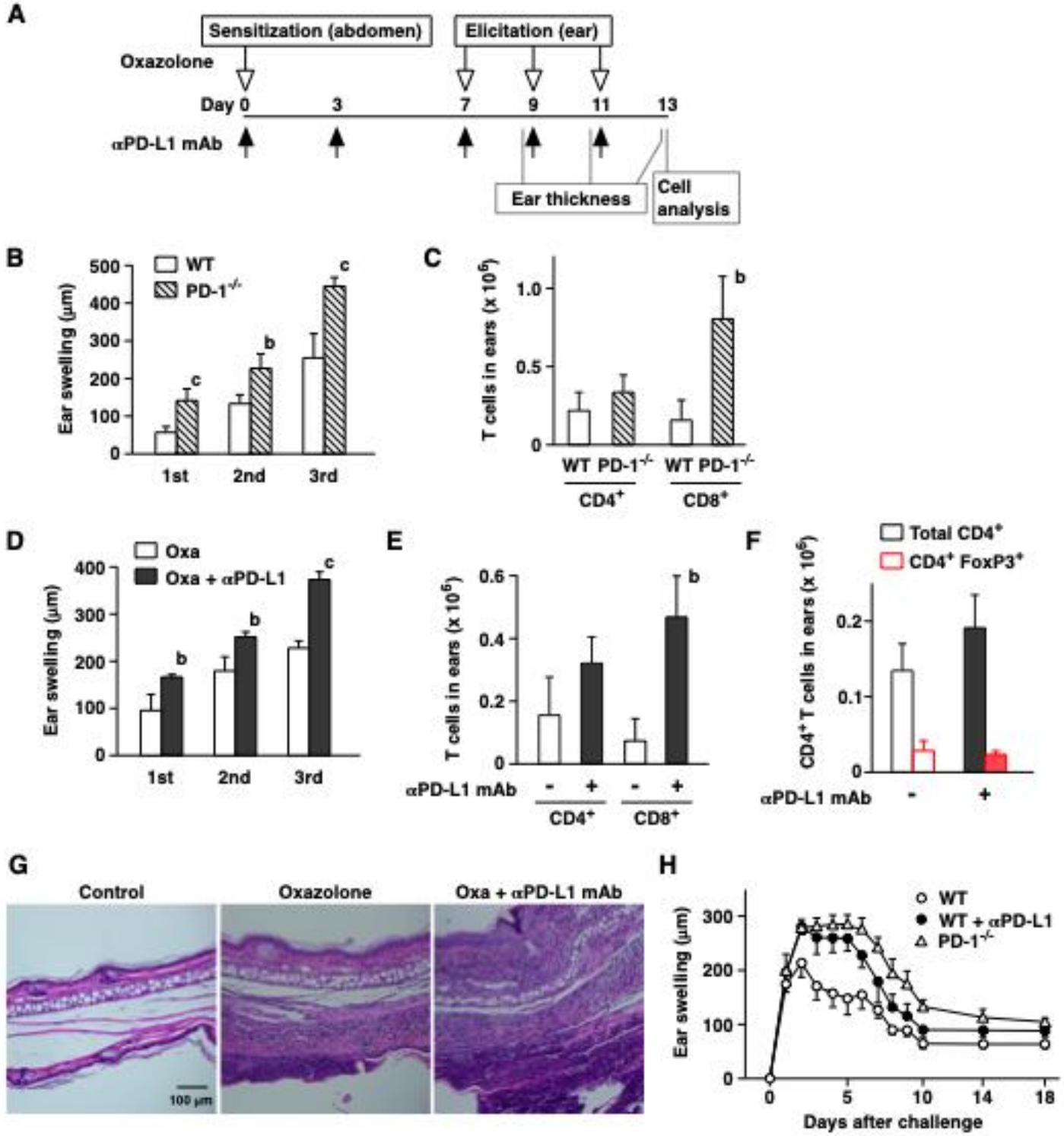
A
Sensitization (abdomen)
Elicitation (ear)
Oxazolone
Day 0
3
7
9
11
13
αPD-L1 mAb
Ear thickness
Cell analysis
B
WT
PD-1-/-
Ear swelling (μm)
1st
2nd
3rd
C
T cells in ears (x 10^6)
WT PD-1-/- WT PD-1-/-
CD4+
CD8+
D
Oxa
Oxa + αPD-L1
Ear swelling (μm)
1st
2nd
3rd
E
T cells in ears (x 10^6)
αPD-L1 mAb
CD4+
CD8+
F
Total CD4+
CD4+ FoxP3+
CD4+ T cells in ears (x 10^6)
αPD-L1 mAb
G
Control
Oxazolone
Oxa + αPD-L1 mAb
100 μm
H
WT
WT + αPD-L1
PD-1-/-
Ear swelling (μm)
Days after challenge

Figure 1

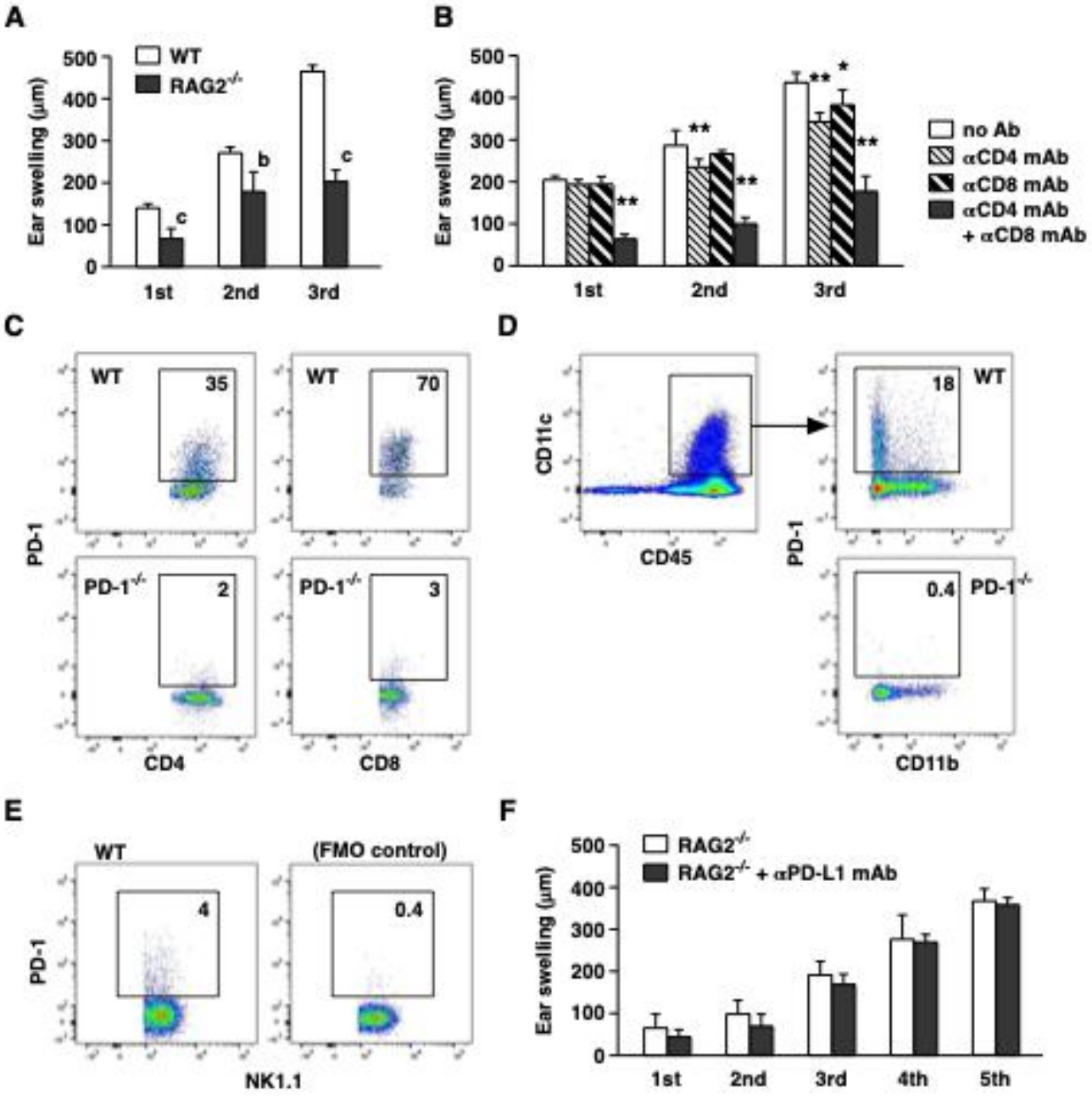
A
WT
RAG2-/-
Ear swelling (μm)
500
400
300
200
100
0
c
b
c
1st
2nd
3rd
B
Ear swelling (μm)
**
**
**
*
**
no Ab
αCD4 mAb
αCD8 mAb
αCD4 mAb
+ αCD8 mAb
1st
2nd
3rd
C
WT
35
WT
70
PD-1
PD-1-/-
2
PD-1-/-
3
CD4
CD8
D
CD11c
CD45
18
WT
PD-1
0.4
PD-1-/-
CD11b
E
WT
(FMO control)
4
0.4
PD-1
NK1.1
F
RAG2-/-
RAG2-/- + αPD-L1 mAb
Ear swelling (μm)
500
400
300
200
100
0
1st
2nd
3rd
4th
5th

Figure 2

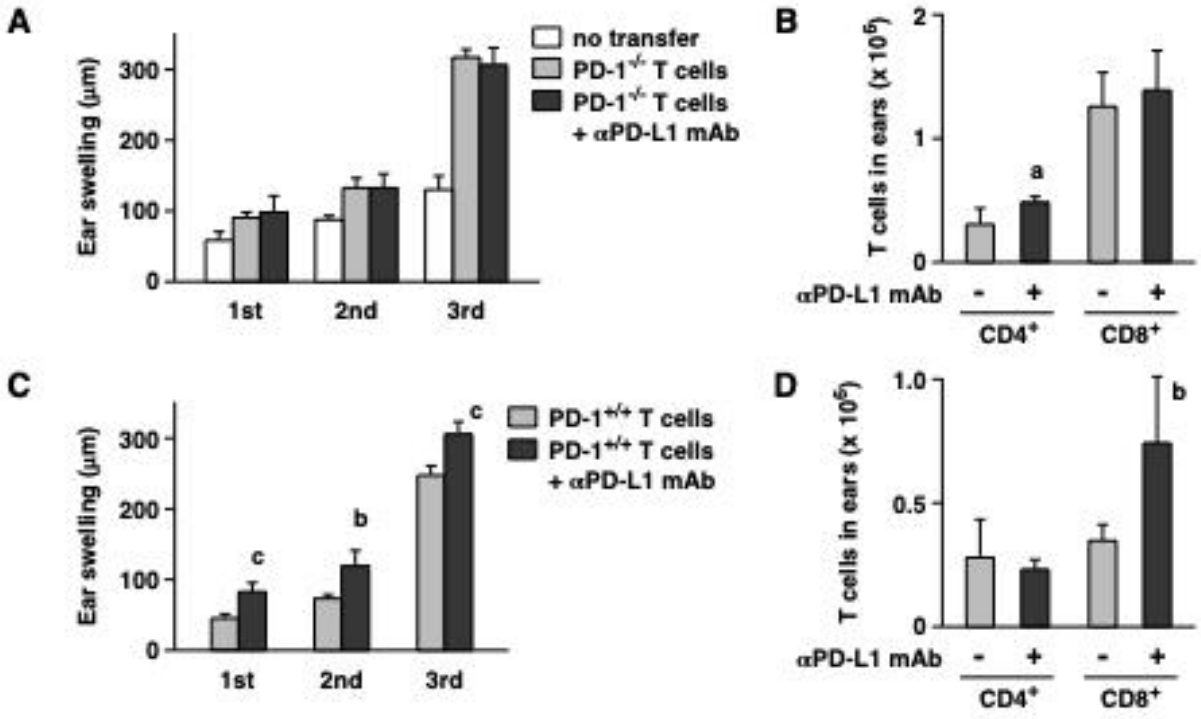
A
Ear swelling (μm)
300
200
100
0
1st
2nd
3rd
no transfer
PD-1-/- T cells
PD-1-/- T cells
+ αPD-L1 mAb
B
T cells in ears (x 10^6)
2
1
0
a
αPD-L1 mAb
-
+
-
+
CD4+
CD8+
C
Ear swelling (μm)
300
200
100
0
c
b
c
1st
2nd
3rd
PD-1+/+ T cells
PD-1+/+ T cells
+ αPD-L1 mAb
D
T cells in ears (x 10^6)
1.0
0.5
0
b
αPD-L1 mAb
-
+
-
+
CD4+
CD8+

Figure 3

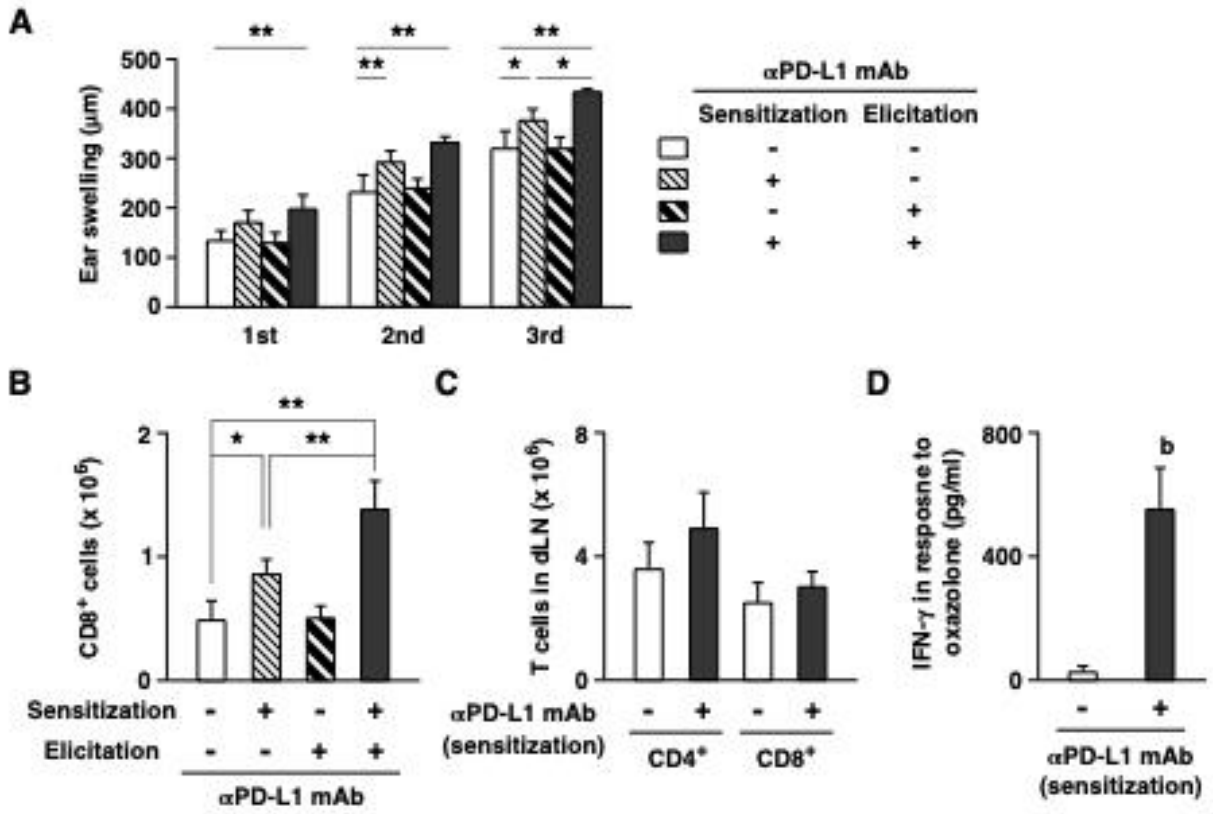
A
Ear swelling (μm)
500
400
300
200
100
0
1st
2nd
3rd
αPD-L1 mAb
Sensitization
Elicitation
B
CD8+ cells (x 10^5)
2
1
0
Sensitization
Elicitation
αPD-L1 mAb
C
T cells in dLN (x 10^6)
8
4
0
αPD-L1 mAb (sensitization)
CD4+
CD8+
D
IFN-γ in response to oxazolone (pg/ml)
800
400
0
b
αPD-L1 mAb (sensitization)

Figure 4

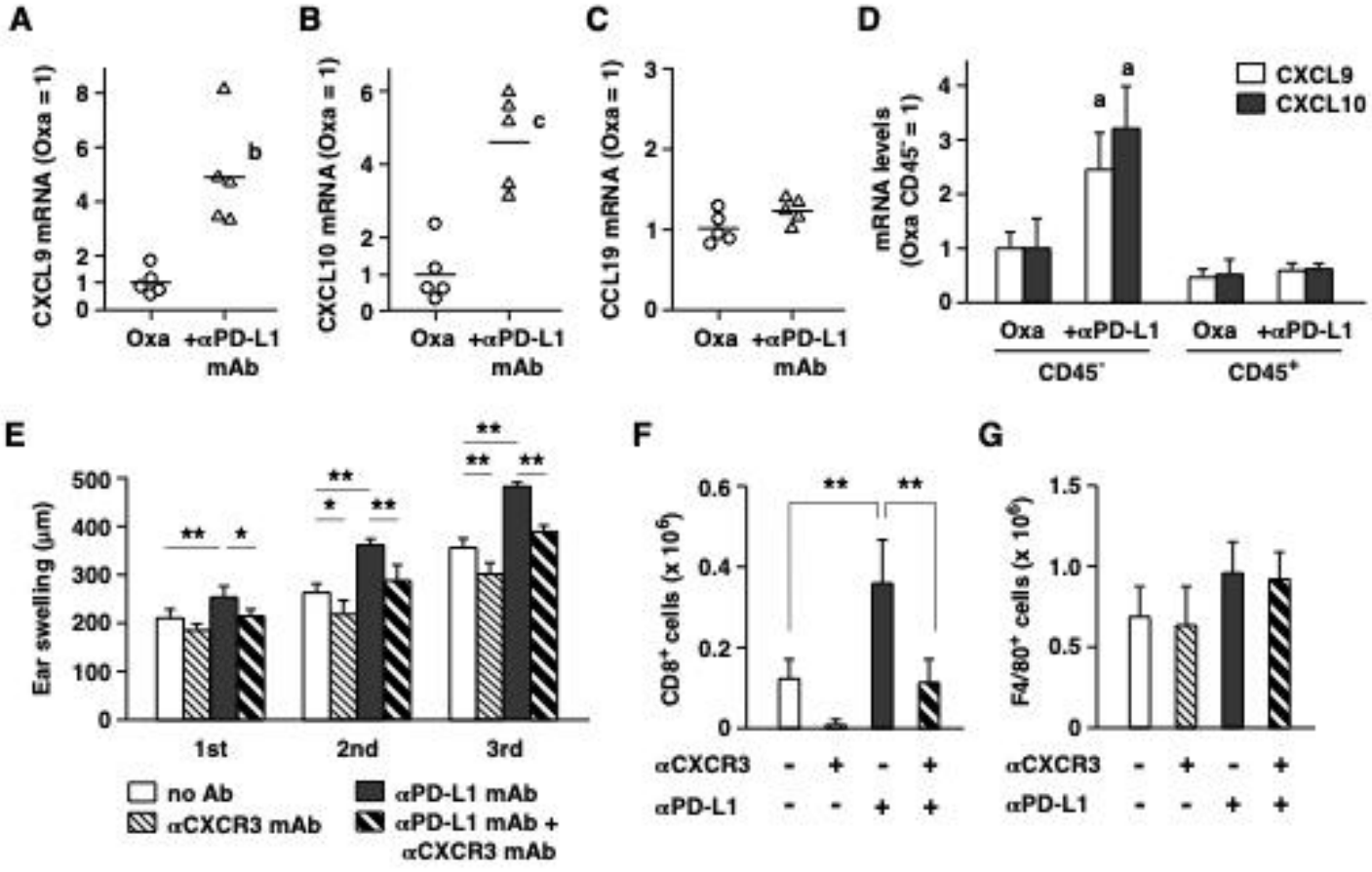
A
CXCL9 mRNA (Oxa = 1)
Oxa
+αPD-L1 mAb
b
B
CXCL10 mRNA (Oxa = 1)
c
C
CCL19 mRNA (Oxa = 1)
D
mRNA levels (Oxa CD45⁻ = 1)
CXCL9
CXCL10
a
CD45⁻
CD45⁺
E
Ear swelling (μm)
1st
2nd
3rd
no Ab
αCXCR3 mAb
αPD-L1 mAb
αPD-L1 mAb + αCXCR3 mAb
F
CD8⁺ cells (x 10⁶)
αCXCR3
αPD-L1
G
F4/80⁺ cells (x 10⁶)

Figure 5

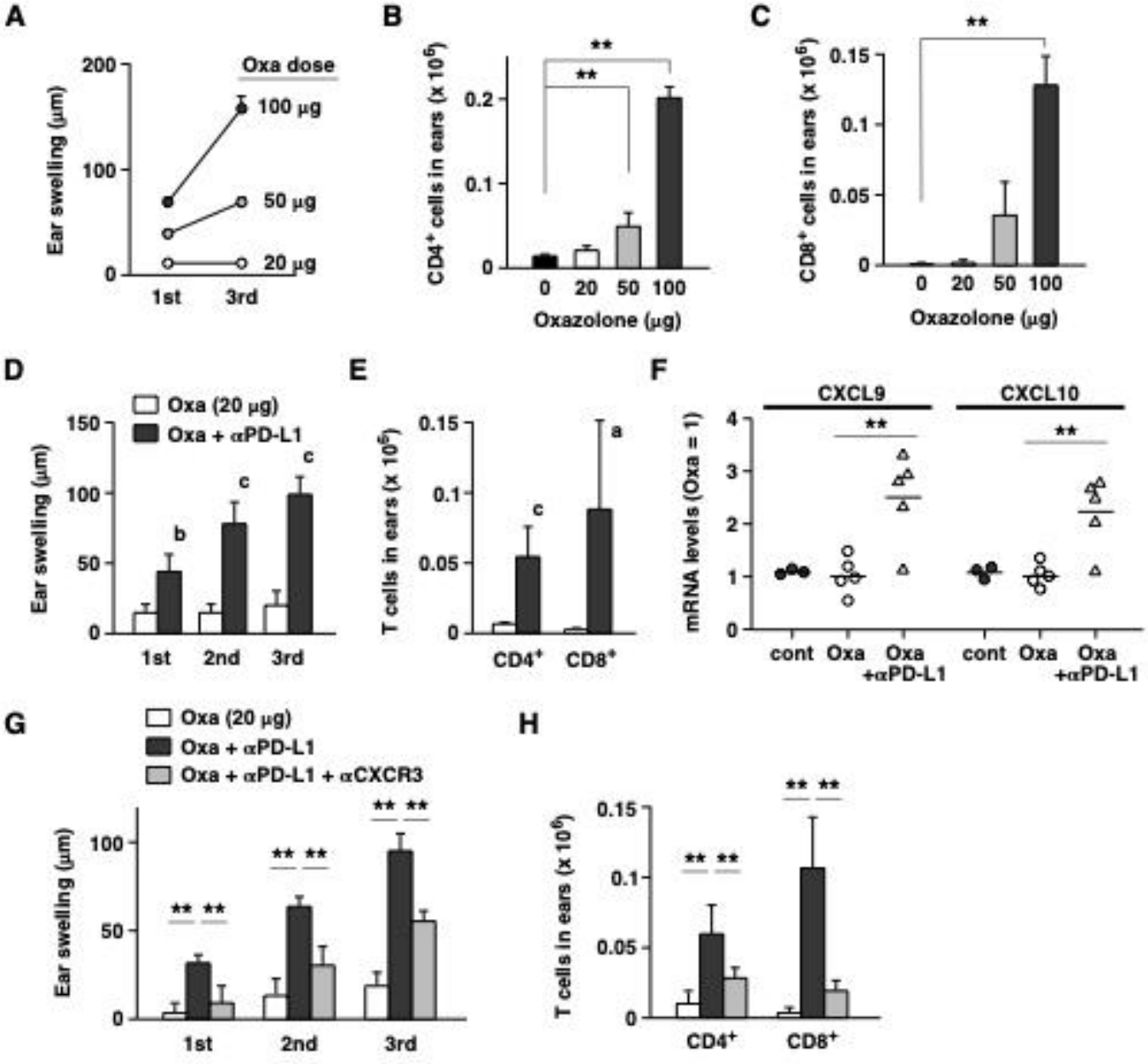
A
Ear swelling (μm)
200
100
0
Oxa dose
100 μg
50 μg
20 μg
1st
3rd
B
CD4+ cells in ears (x 10^5)
0.2
0.1
0
**
**
0 20 50 100
Oxazolone (μg)
C
CD8+ cells in ears (x 10^5)
0.15
0.1
0.05
0
**
0 20 50 100
Oxazolone (μg)
D
Oxa (20 μg)
Oxa + αPD-L1
Ear swelling (μm)
150
100
50
0
b
c
c
1st 2nd 3rd
E
T cells in ears (x 10^5)
0.15
0.1
0.05
0
c
a
CD4+ CD8+
F
CXCL9
CXCL10
mRNA levels (Oxa = 1)
4
3
2
1
0
**
**
cont Oxa Oxa +αPD-L1 cont Oxa Oxa +αPD-L1
G
Oxa (20 μg)
Oxa + αPD-L1
Oxa + αPD-L1 + αCXCR3
Ear swelling (μm)
100
50
0
** **
** **
** **
1st 2nd 3rd
H
T cells in ears (x 10^6)
0.15
0.1
0.05
0
** **
** **
CD4+ CD8+

Figure 6